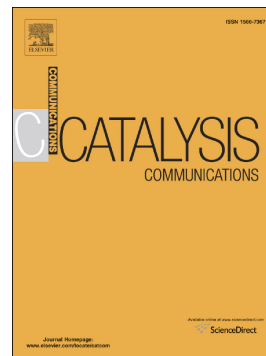


Accepted Manuscript

Stabilized Cu/Cu₂O nanoparticles on rGO as an efficient heterogeneous catalyst for Glaser homo-coupling

Weiyang Lu, Wei Sun, Xiaofeng Tan, Lingfeng Gao, Gengxiu Zheng



PII: S1566-7367(19)30110-4
DOI: <https://doi.org/10.1016/j.catcom.2019.04.002>
Reference: CATCOM 5670
To appear in: *Catalysis Communications*
Received date: 2 January 2019
Revised date: 30 March 2019
Accepted date: 1 April 2019

Please cite this article as: W. Lu, W. Sun, X. Tan, et al., Stabilized Cu/Cu₂O nanoparticles on rGO as an efficient heterogeneous catalyst for Glaser homo-coupling, *Catalysis Communications*, <https://doi.org/10.1016/j.catcom.2019.04.002>

This is a PDF file of an unedited manuscript that has been accepted for publication. As a service to our customers we are providing this early version of the manuscript. The manuscript will undergo copyediting, typesetting, and review of the resulting proof before it is published in its final form. Please note that during the production process errors may be discovered which could affect the content, and all legal disclaimers that apply to the journal pertain.

Stabilized Cu/Cu₂O nanoparticles on rGO as an efficient heterogeneous catalyst for Glaser homo-coupling

Weiyang Lu^a, Wei Sun^a, Xiaofeng Tan^a, Lingfeng Gao^{a,*} gaolf108@mail.ustc.edu.cn and
Gengxiu Zheng^{a,*} chm_zhenggx@ujn.edu.cn

^aSchool of Chemistry and Chemical Engineering, University of Jinan, Jinan, Shandong 250022, China

Corresponding authors.

Abstract

Stabilized Cu/Cu₂O nanoparticles on reduced graphene oxide (Cu/Cu₂O-NPs@rGO) was synthesized by one-step co-reduction and acted as a green and efficient non-noble metal heterogeneous catalyst for Glaser homo-coupling. Through the synergic catalytic effect of Cu/Cu₂O nanoparticles and graphene, the heterogeneous hybrid nanoparticles catalyst showed excellent catalytic performance for Glaser homo-coupling with the yield up to 99% of 1,4-diphenyl buta-1,3-diyne. And excellent functional group tolerance was obtained with oxygen as a green oxidant. Furthermore, the catalyst can be easily separated and recycled seven times without significant decline in its catalytic performance.

Keywords: Cu/Cu₂O nanoparticles; graphene; Glaser homo-coupling; heterogeneous hybrid catalyst; oxygen

1. Introduction

1,3-Diynes have both symmetric and unsymmetric structures with the properties of anti-inflammatory, anti-bacterial, and anti-cancer activities. These compounds widely exist in numerous pharmaceuticals and bioactive molecules[1-4]. They are also useful precursors in the synthesis of functional materials because the unsaturated alkynyl group could further involve in many kinds of reactions[5-7]. Therefore, it is of great significance to develop an excellent catalyst for the synthesis of 1,3-diynes.

Glaser homo-coupling is one of the most classical reaction for the synthesis of symmetric 1,3-diynes[8]. The reaction was generally carried out on homogeneous systems, in which copper salts or palladium salts were frequently used as catalyst[9, 10]. Typical disadvantages of homogeneous systems were the difficulties in the recyclability of catalyst and product contamination caused by heavy metal residue resulting in their difficulties in industrial application. To overcome these problems, some of efficient heterogeneous catalysts have been investigated, such as Au/CeO₂[11], Au@NH₂-SBA-15[12], Au/La₂O₃[13], AgNPs@g-C₃N₄[14]. Most of these catalysts used the noble metal with the high cost and multi-step synthesis processes. Thus, developing efficient no-noble metal heterogeneous catalyst with the simple synthetic process is of great value for practical applications in Glaser homo-coupling reaction.

Among the transition metal nanomaterials, Cu-NPs (e.g., Cu, Cu₂O, or CuO) materials have always attracted more attention as the catalyst than others because of copper's low cost, abundant reserves, outstanding physical and chemical properties[15]. However, the inherent drawback of Cu⁰/Cu⁺-NPs was easily oxidized under atmospheric conditions, limiting their practical application[16]. Graphene, as a single layer of sp² bonded carbon material[17], possesses many advantages such as

superior electroconductive performances[18, 19], large surface area, excellent thermal and chemical stability[20]. The unique properties facilitated its use in photoelectric devices[21, 22], energy storage[23, 24], chemical sensor[25, 26] as well as an ideal support for high performance catalysts[27, 28]. For the synthesis of highly active catalysts, we combined both the advantages of Cu-NPs and graphene. The formation of Cu/Cu₂O-NPs@rGO made the Cu/Cu₂O-NPs well dispersed and stabilized on the surface of rGO. By this method, Cu/Cu₂O-NPs were endowed with great anti-aggregation and excellent stability, then further applied in the field of organic catalysis.

In our previous work, we have developed a green and economical Cu NPs-based catalyst for the oxidation of alcohols to aldehydes with high conversion and selectivity[29]. Then we further developed a sustainable heterogeneous catalyst Cu/Cu₂O-NPs@rGO for Glaser homo-coupling. By the π - π stacking interaction between phenylacetylene and rGO layers[30], the alkynyl groups were enriched around the rGO to further accelerate the reaction rate. As a result, our new designed hybrid Cu/Cu₂O nanoparticles on reduced graphene oxide (Cu/Cu₂O-NPs@rGO) shows excellent catalysis for Glaser homo-coupling. Meanwhile, Cu/Cu₂O-NPs@rGO could be easily separated by centrifugation and reused seven times without significant decline in its catalytic performance.

2. Experimental

2.1. Graphene Oxide(GO) preparation

Graphene oxide (GO) was prepared by modified Hummers method through the intense oxidation of natural graphite powder and then ultrasonic stripping. The prepared details are given in the Supporting Information.

2.2. Synthesis of Cu/Cu₂O-NPs@rGO catalysts

The Cu/Cu₂O-NPs@rGO catalysts were prepared as follow: The as-prepared GO was dispersed into deionized water getting GO solution of 2 mg·mL⁻¹. 10 mL of Cu(OAc)₂·H₂O (0.2 mol·mL⁻¹) was mixed with 50 mL of GO (2 mg·mL⁻¹) under constant magnetic stirring to get an evenly mixture. Subsequently, 10 mL of ascorbic acid (VC) aqueous solution (0.4 mol/L) was added to the mixture slowly. Then, the mixture was stirred for 2 h at 60 °C. After the reaction was finished, the reaction solution was cooled to room temperature naturally. The Cu/Cu₂O-NPs@rGO catalyst was centrifuged out from the reaction solution, washed with water and ethanol, and dried in a lyophilization step. The rGO was synthesized by the same way without Cu(OAc)₂·H₂O.

2.3. Characterization

The prepared Cu/Cu₂O-NPs@rGO samples were characterized by XRD, XPS, N₂-BET, ICP, SEM, TEM. More details about these characterizations are given in Supporting Information.

2.4. Typical experimental process for Glaser homo-coupling

Glaser homo-coupling reaction was evaluated in a 25 mL round bottomed flask under constant magnetic stirring. Typically, a mixture of phenylacetylene (1 mmol), catalyst, base and solvent (2 mL) were added into round the bottomed flask. Subsequently O₂ was introduced into the reaction system instead of air. The mixture solution was stirred at 80 °C for 8 h. After the reaction was finished, the reaction solution was cooled down to room temperature naturally. The solid catalyst was centrifuged recovered and organic phase was extracted with ethyl acetate to get crude products. All crude products were purified by column chromatography to calculate the yields and identified by ¹H NMR and ¹³C NMR spectra.

3. Results and discussion

3.1. Characterization of Cu/Cu₂O-NPs@rGO

[Insert **Fig. 1**]

The typical XRD diffraction pattern of Cu/Cu₂O-NPs@rGO was presented in Fig. 1 a. The diffraction peaks at 29.6, 36.5, 42.4, 61.5 can be assigned to the (110), (111), (200), (220) planes of cubic Cu₂O crystal phase (JCPDS No. 65-3288). And strong diffraction peaks at 43.3, 50.4, 74.1 were well consistent with the (111), (200), (220) planes of cubic Cu crystal phase (JCPDS No. 04-0836) while no diffraction peaks of other impurities were observed. The results indicated that the Cu/Cu₂O nanoparticles had the high crystallinity. XPS was conducted to analyze the oxidation state of Cu on the surface of graphene. The result was shown in Fig. 1 b. The binding energy located at approximately 932.5 eV and satellite peaks at 952.5 eV can be assigned to Cu⁰/Cu⁺ because there is only a difference of 0.1-0.2 eV between the binding energies of Cu⁰ and Cu⁺[30]. The much lower peak at 934.9 eV and satellite peaks at 943.2 eV were attributed to Cu(OH)₂ (Cu²⁺) in Cu/Cu₂O-NPs@rGO[31] because a small part of Cu²⁺ was incomplete reduced[29]. And the XRD pattern clearly indicated that the formation of Cu/Cu₂O crystals without the presence of CuO crystals. ICP-OES was used to detect total amount of Cu in the catalyst and the result was 26.24 w. t. %. The above characterization results indicated that Cu/Cu₂O nanoparticles were successfully generated with highly crystalline.

[Insert **Fig. 2**]

The morphology and structure of Cu/Cu₂O-NPs@rGO were characterized by TEM and SEM. From the TEM image of Fig. 2 a, oxygen-containing groups (such as hydroxyl, epoxy, and carboxyl group) on the surface of GO can act as anchoring sites for the formation of metal nanoparticles[32]. And we could see that a lot of dark

Cu/Cu₂O nanoparticles were distributed evenly on the surface of transparent films-like rGO. Further, the typical wrinkle structures were still exhibited on the surface of Cu/Cu₂O-NPs@rGO, which demonstrated that the layered structure of the catalyst was unchanged by one-step co-reduction. From the SEM image of Fig. 2 b, it could be seen that some bright nanoparticles supported well on the wrinkled surface of the rGO. The consistency of both TEM and SEM images suggested that Cu/Cu₂O nanoparticles were successfully loaded on the rGO. Moreover, the N₂-BET result was shown in Fig. S4. and Fig. S5. the S_{BET} of the Cu/Cu₂O-NPs@rGO was obtained as 100 m²·g⁻¹, and the average pore diameter of Cu/Cu₂O-NPs@rGO was 11.9 nm.

3.2. Catalytic performance

At the beginning of the experiment, the Glaser homo-coupling was carried out in EtOH with various catalysts under O₂ at 80 °C for 8 h. And the catalytic performance is summarized in Table 1. In the absence of catalyst, the homo-coupling of phenylacetylene was inhibited (Table 1, entry 1). It was indicated that the reaction was very difficult to carry out without any catalyst. Several copper salts exhibited moderate catalytic activities. (Table 1, entries 2, 3). Cu-NPs, Cu₂O-NPs and CuO-NPs were also investigated in the experiment. It could be seen that Cu-NPs showed relatively higher catalytic activity compared with Cu₂O-NPs and CuO-NPs at the yield of 81% (Table 1, entries 5-7). The mixed catalyst of Cu-NPs and Cu₂O-NPs of equal mass ratio only gave the yield of 80% (Table 1, entry 8). In addition, rGO exhibited little catalytic activity (Table 1, entry 9). With the extension of reaction time, the yield of 1,4-diphenyl buta-1,3-diyne was also increased (Table 1, entries 10-12, for details, see Fig. S2). Notably, when the reaction time reached 8 hours, Cu/Cu₂O-NPs@rGO gave excellent catalytic activity for the homo-coupling of phenylacetylene with the yield up to 99% (Table 1, Entry 11). Besides, when the

dosage of phenylacetylene was increased to 10 mmol, the yield was 96% and no significant loss in the yield was observed (Table 1, Entry 13). It was proved that the Cu/Cu₂O-NPs@rGO had outstanding potential in industrial application. The above results indicated that the synergic catalytic effect of Cu/Cu₂O nanoparticles and rGO significantly improved the catalytic activity for the Glaser homo-coupling.

[Insert **Table 1**]

Then, various solvents were evaluated for the Glaser homo-coupling. And the results were shown in Table S1. When some polar solvents such as DMF, DMSO, CH₃CN were utilized as solvents, low yields were observed (6-42%, Table S1, entries 1-3). Then some non-polar solvents were investigated in the reaction such as CH₂Cl₂, THF and toluene, low yields were also obtained (0-32%, Table S1, entries 4-6). Through experiment and observation, we found that the Cu/Cu₂O-NPs@rGO had poor dispersion in the solvents of CH₂Cl₂, THF and toluene. Because phenylacetylene and H₂O were incompatible, the reaction was even almost inhibited in H₂O (Table S1, entry 10). To our delight, when alcohols were used as solvent, the good to excellent yields of the homo-coupling of phenylacetylene were obtained (Table S1, entries 7-9). Especially in EtOH solvent, the yield was up to 99%. Based on the above results, alcohols solvents were propitious to the Glaser homo-coupling reaction. For the convenience of handing, EtOH (2 mL) was utilized as the solvent.

Moreover, Fig. S1 indicated that the optimum reaction temperature on the homo-coupling of phenylacetylene over the Cu/Cu₂O-NPs@rGO was 80 °C. Different bases were also optimized for the Glaser homo-coupling and Cs₂CO₃ is the best choice (for details, see Table. S2). Thus, the optimal reaction parameters were obtained as following: 1 mmol of phenylacetylene, 4 mg of Cu/Cu₂O-NPs@rGO and 1.2 mmol of Cs₂CO₃ in 2 mL EtOH at 80 °C under O₂ for 8 h.

Under the optimum reaction conditions, we have investigated a series of functional groups on phenylacetylene including electron-donating groups and electron-withdrawing groups. All of them gave good to excellent yields. The phenylacetylene bearing withdrawing groups F-, Cl- and Br- offered higher yields of 94%, 98%, 96% respectively (Table 2, entries 2-4). The phenylacetylene bearing donating groups offered the high yields (CH_3CH_2 -: 92%, $(\text{CH}_3)_3\text{C}$ -: 91%, $\text{CH}_3(\text{CH}_2)_3\text{CH}_2$ -: 90%, CH_3O -: 94%, NH_2 -: 85%) (Table 2, entries 5-9). The heterocyclic substrates were also examined in the reaction condition, giving good yields of 83% and 94% (Table 2, entries 10, 11). Hexadeca-7,9-diyne was also investigated in the reaction with a moderate yield of 53% (Table 2, entry 12). The above results revealed that the Cu/Cu₂O-NPs@rGO exhibited excellent catalytic activity for Glaser homo-coupling of both aromatic and heterocyclic alkynes, and possessed excellent functional groups tolerance.

[Insert Table 2]

According to the previous reports[33-35] and our studies, a proposed mechanism was shown in Fig. 3. Due to the strong electric conduction of graphene, the value states of Cu/Cu₂O-NPs were easily changed by electron transfer. Also, the presence of the huge surface of rGO and a number of exposed Cu/Cu₂O nanoparticles facilitated the homo-coupling of the terminal alkynes. First, by the π - π stacking interaction between aromatic ring and rGO layers, the alkynyl groups were enriched around the rGO to coordinate with exposed Cu/Cu₂O nanoparticles on the rGO and generated **I**. The inactive C-H bond was activated for active C-H bond. Under the alkaline condition of Cs₂CO₃, **I** was deprotonated, C-Cu/Cu₂O-NPs@rGO bond was formed obtaining **II**. **II** were dimerized affording **III**. Subsequently, **III** taken part in the electron transfer promoted by good conductive Cu/Cu₂O-NPs@rGO and C-C bond

was then formed to obtain the final product 1,3-diyne with realizing the Cu/Cu₂O-NPs@rGO for the next catalysis cycle. Along with the catalysis process, the transformation of Cu(0) and Cu (I) on the rGO was realized by the oxidation of O₂.

[Insert **Fig. 3**]

Recyclability is an imperative aspect of heterogeneous catalytic performance. The recyclability of the Cu/Cu₂O-NPs@rGO was investigated with the phenylacetylene as standard substrate under optimal conditions. Cu/Cu₂O-NPs@rGO was recycled seven times after easily separated by centrifugation and washed with ethanol and water. And the result was shown in Fig. S3. There was no evident decline in its catalytic activities after seven times with the yield of 92%. Moreover, the XRD pattern of the recycled Cu/Cu₂O-NPs@rGO was shown in Fig. S6. The diffraction peaks of cubic Cu and Cu₂O were highly consistent with Fig. 1 a. It indicated that the catalyst had no obvious change after recycled for seven consecutive times.

4. Conclusions

In summary, we have developed an efficient heterogeneous catalyst Cu/Cu₂O-NPs@rGO for Glaser homo-coupling. The Cu/Cu₂O-NPs@rGO was prepared by simple chemical co-reduction and had some advantages such as green catalytic system, high catalytic activity, easy separation and excellent recyclability. After a series of characterizations of XRD, XPS, N₂-BET, ICP, SEM, TEM, Cu/Cu₂O nanoparticles were proved to firmly support on the rGO. Cu/Cu₂O-NPs@rGO successfully catalyzed the homo-coupling of various terminal alkynes with good to excellent yields. Our results provide a reliable method for configuring copper-based carbon catalysts and more opportunities for heterogeneous catalytic applications in organic reaction.

Acknowledgements

This study was supported by the Natural Science Foundation of Shandong Province (ZR2017PB005) and the National Natural Science Foundation of China (Nos. 21601064).

Appendix A. Supplementary data

Supplementary data to this article can be found online at: **please add the website.**

ACCEPTED MANUSCRIPT

References

- [1] W. Yin, C. He, M. Chen, H. Zhang, A. Lei, Nickel-catalyzed oxidative coupling reactions of two different terminal alkynes using O₂ as the oxidant at room temperature: facile syntheses of unsymmetric 1,3-diynes, *Org. Lett.*, 11 (2009) 709-712.
- [2] D. Lechner, M. Stavri, M. Oluwatuyi, R. Pereda-Miranda, S. Gibbons, The anti-staphylococcal activity of angelica dahurica (Bai Zhi), *Phytochemistry*, 65 (2004) 331-335.
- [3] L. Su, J. Dong, L. Liu, M. Sun, R. Qiu, Y. Zhou, S. Yin, Copper catalysis for selective heterocoupling of terminal alkynes, *J. Am. Chem. Soc.*, 138 (2016) 12348-12351.
- [4] K. S. Sindhu, G. Anilkumar, Recent advances and applications of Glaser coupling employing greener protocols, *RSC Adv.*, 4 (2014) 27867-27887.
- [5] J. Liu, J. W. Y. Lam, B. Z. Tang, Acetylenic polymers: syntheses, structures, and functions, *Chem. Rev.*, 109 (2009) 5799-5867.
- [6] W. Shi, A. Lei, 1,3-Diyne chemistry: synthesis and derivations, *Tetrahedron Lett.*, 55 (2014) 2763-2772.
- [7] L. Su, J. Dong, L. Liu, M. Sun, R. Qiu, Y. Zhou, S. Yin, Copper catalysis for selective heterocoupling of terminal alkynes, *J. Am. Chem. Soc.*, 138 (2016) 12348-12351.
- [8] C. Glaser, Beiträge zur kenntniss des acetenylbenzols, *Ber. Dtsch. Chem. Ges.*, 2 (1869) 422-424.
- [9] W. Zhang, W. Xu, F. Zhang, G. Qu, Synthesis of symmetrical 1,3-diynes via tandem reaction of (Z)-arylvinyl bromides in the presence of DBU and CuI, *Chin. Chem. Lett.*, 24 (2013) 407-410.

- [10] L. Li, J. Wang, G. Zhang, Q. Liu, A mild copper-mediated Glaser-type coupling reaction under the novel CuI/NBS/DIPEA promoting system, *Tetrahedron Lett.*, 50 (2009) 4033-4036.
- [11] G. Camino, A. Alberto, C. Avelino, G. Hermenegildo, I. Marta, S. Félix, Catalysis by gold(I) and gold(III): A parallelism between homo- and heterogeneous catalysts for copper-free sonogashira cross-coupling reactions, *Angew. Chem. Int. Ed.*, 46 (2007) 1536-1538.
- [12] B. Vilhanová, J. Václavík, L. Artiglia, M. Ranocchiari, A. Togni, J. A. V. Bokhoven, Subnanometer gold clusters on amino-functionalized silica: An efficient catalyst for the synthesis of 1,3-diynes by oxidative alkyne coupling, *ACS Catal.*, 7 (2017) 3414-3418.
- [13] S. K. Beaumont, G. Kyriakou, R. M. Lambert, Identity of the active site in gold nanoparticle-catalyzed sonogashira coupling of phenylacetylene and iodobenzene, *J. Am. Chem. Soc.*, 132 (2010) 12246-12248.
- [14] S. B. Patel, D. V. Vasava, Carbon nitride-supported silver nanoparticles: microwave assisted synthesis of propargylamine and oxidative C-C coupling reaction, *Chemistry Select*, 3 (2018) 471-480.
- [15] J. Zhang, J. Liu, Q. Peng, X. Wang, Y. Li, Nearly monodisperse Cu₂O and CuO nanospheres: preparation and applications for sensitive gas sensors, *Chem. Mater.*, 18 (2006) 867-871.
- [16] M. B. Gawande, A. Goswami, F. X. Felpin, T. Asefa, X. Huang, R. Silva, X. Zou, R. Zboril, R. S. Varma, Cu and Cu-based nanoparticles: synthesis and applications in catalysis, *Chem. Rev.*, 116 (2016) 3722-3811.
- [17] J. Balamurugan, T. D. Thanh, S. B. Heob, N. H. Kima, J. H. Lee, Novel route to synthesis of N-doped graphene/Cu-Ni oxide composite for high electrochemical

performance, *Carbon*, 94 (2015) 962-970.

[18] Y. J. Yao, Y. M. Cai, F. Lu, F. Y. Wei, X. Y. Wang, S. B. Wang, Magnetic recoverable MnFe_2O_4 and MnFe_2O_4 -graphene hybrid as heterogeneous catalysts of peroxymonosulfate activation for efficient degradation of aqueous organic pollutants, *J. Hazard. Mater.*, 270 (2014) 61-70.

[19] Y. J. Yao, S. D. Miao, S. Z. Liu, L. P. Ma, H. Q. Sun, S. B. Wang, Synthesis characterization, and adsorption properties of magnetic Fe_3O_4 @graphene nanocomposite, *Chem. Eng. J.*, 184 (2012) 326-332.

[20] P. Kumar, F. Shahzad, S. Yu, S. M. Hong, Y.-H. Kim, C. M. Koo, Large-area reduced graphene oxide thin film with excellent thermal conductivity and electromagnetic interference shielding effectiveness, *Carbon*, 94 (2015) 494-500.

[21] L. Yang, L. Wang, M. Xing, J. Lei, J. Zhang, Silica nanocrystal/graphene composite with improved photoelectric and photocatalytic performance, *Appl. Catal. B-Environ.*, 180 (2016) 106-112.

[22] Y. Zhou, E. Yiwen, L. Zhu, M. Qi, X. Xu, J. Bai, Z. Ren, L. Wang, Terahertz wave reflection impedance matching properties of graphene layers at oblique incidence, *Carbon*, 96 (2015) 1129-1137.

[23] C. Xu, B. Xu, Y. Gu, Z. Xiong, J. Sun, X. S. Zhao, Graphene-based electrodes for electrochemical energy storage, *Energ. Environ. Sci.*, 6 (2013) 1388-1414.

[24] Y. Yang, L. Li, H. Fei, Z. Peng, G. Ruan, J. M. Tour, Graphene nanoribbon/ V_2O_5 cathodes in Lithium-Ion batteries, *ACS Appl. Mater. Interfaces*, 6 (2014) 9590-9594.

[25] R. Furue, E. P. Koveke, S. Sugimoto, Y. Shudo, S. Hayami, S. I. Ohira, K. Toda, Arsine gas sensor based on gold-modified reduced graphene oxide. *Sens. Actuators, B*, (240) 2017 657-663.

[26] G. J. Rani, K. J. Babu, G. G. kumar, M. A. J. Rajan, *Watsonia meriana* flower like

Fe₃O₄/reduced graphene oxide nanocomposite for the highly sensitive and selective electrochemical sensing of dopamine, *J. Alloys Compd.*, 688 (2016) 500-512.

[27] M. Hu, Z. Yao, K. N. Hui, K. S. Hui, Novel mechanistic view of catalytic ozonation of gaseous toluene by dual-site kinetic modelling, *Chem. Eng. J.*, 308 (2017) 710-718.

[28] M. A. Al-Daous, Graphene-MoS₂ composite: hydrothermal synthesis and catalytic property in hydrodesulfurization of dibenzothiophene, *Catal. Commun.*, 72 (2015) 180-184.

[29] X. Feng, P. Lv, W. Sun, X. Han, L. Gao, G. Zheng, Reduced graphene oxide-supported Cu nanoparticles for the selective oxidation of benzyl alcohol to aldehyde with molecular oxygen, *Catal. Commun.*, 99 (2017) 105-109.

[30] K. Yang, Y. Yan, H. Wang, Z. Sun, W. Chen, H. Kang, Y. Han, W. Zahng, X. Sun, Z. Li, Monodisperse Cu/Cu₂O@C Core-Shell nanocomposite supported on rGO layers as an efficient catalyst derived from Cu-Based MOFs/GO structure, *Nanoscale*, 10 (2018), 17647-17655.

[31] C. Cheng, C. Zhang, X. Gao, Z. Zhuang, C. Du, W. Chen, 3D network and 2D paper of reduced graphene oxide/Cu₂O composite for electrochemical sensing of hydrogen peroxide, *Anal. Chem.*, 90 (2018) 1983-1991.

[32] Y. Gao, D. Ma, C. Wang, J. Guan, X. Bao, Reduced graphene oxide as a catalyst for hydrogenation of nitrobenzene at room temperature, *Chem. Commun.*, 47 (2011) 2432-243.

[33] N. Mizuno, K. Kamata, Y. Nakagawa, T. Oishi, K. Yamaguchi, Scope and reaction mechanism of an aerobic oxidative alkyne homocoupling catalyzed by a di-copper-substituted silicotungstate, *Catal. Today*, 157 (2010) 359-363.

[34] R. Bai, G. Zhang, H. Yi, Z. Huang, X. Qi, C. Liu, J. T. Miller, A. J. Kropf, E. E.

Bunel, Y. Lan, A. Lei, Cu(II)-Cu(I) synergistic cooperation to lead the alkyne C-H activation, *J. Am. Chem. Soc.*, 136 (2014) 16760-16763.

[35] G. Zhang, H. Yi, G. Zhang, Y. Deng, R. Bai, H. Zhang, J. T. Miller, A. J. Kropf, E. E. Bunel, A. Lei, Direct observation of reduction of Cu(II) to Cu(I) by terminal alkynes, *J. Am. Chem. Soc.*, 136 (2014) 924-926.

ACCEPTED MANUSCRIPT

List of Tables & Figures

Table captions

Table 1. The catalytic performance of different catalysts for the Glaser homo-coupling

Table 2. Cu/Cu₂O-NPs@rGO catalysed homo-coupling of various terminal alkynes

Figure captions

Fig. 1. Characterization of Cu/Cu₂O-NPs@rGO (a) XRD pattern; (b) XPS survey spectra

Fig. 2. Characterization of Cu/Cu₂O-NPs@rGO (a) TEM image; (b) SEM image

Fig. 3. Proposed mechanism for Cu/Cu₂O-NPs@rGO catalyzed Glaser homo-coupling

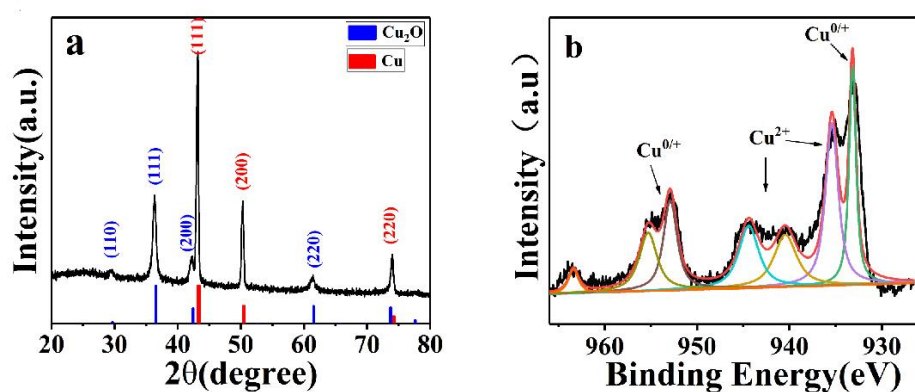


Fig. 1 Characterization of Cu/Cu₂O-NPs@rGO (a) XRD pattern; (b) XPS survey spectra

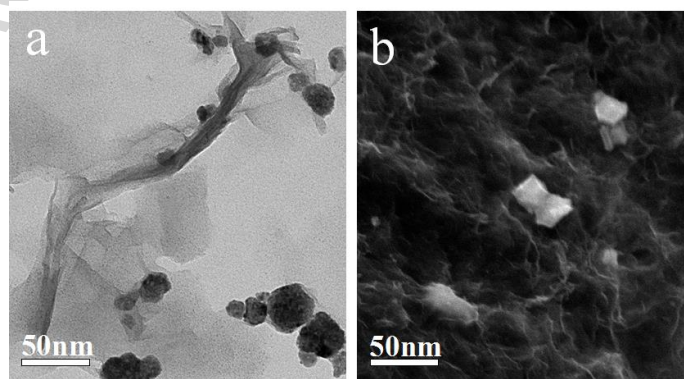


Fig. 2 Characterization of Cu/Cu₂O-NPs@rGO (a) TEM image; (b) SEM image

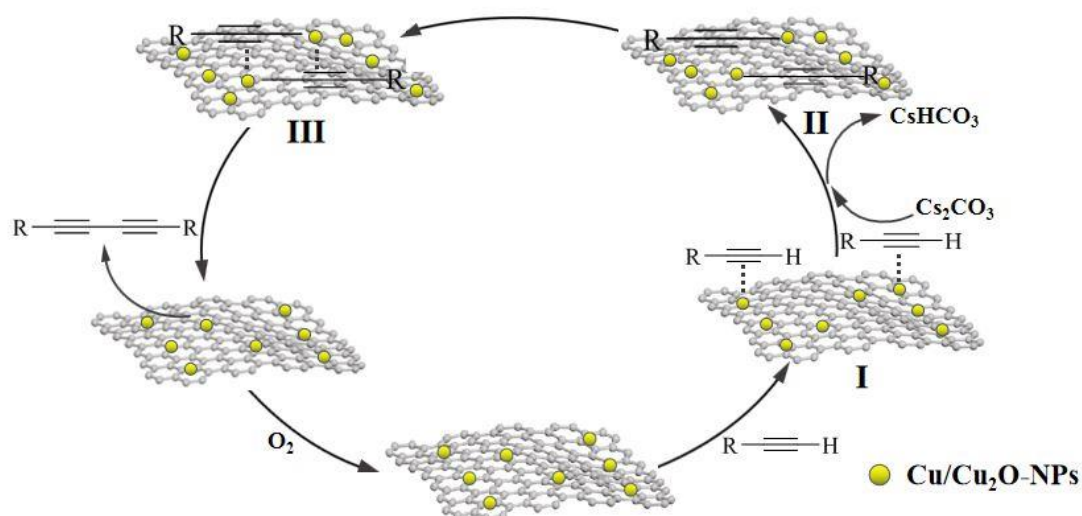


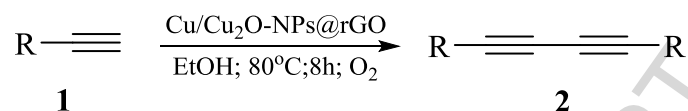
Fig. 3. Proposed mechanism for Cu/Cu₂O-NPs@rGO catalyzed Glaser homo-coupling

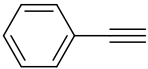
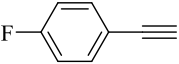
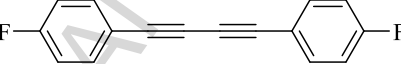
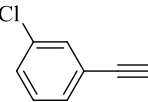
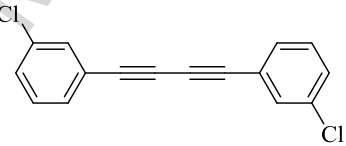
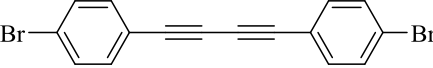
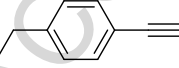
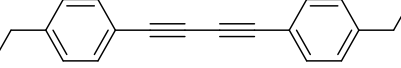
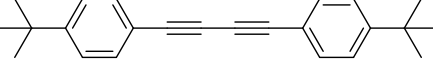
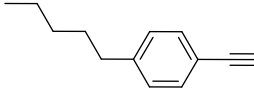
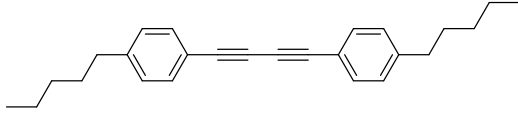
Table 1 The catalytic performance of different catalysts for the Glaser homo-coupling^a

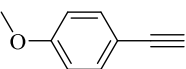
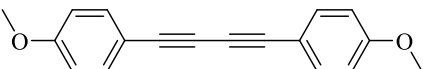
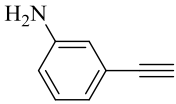
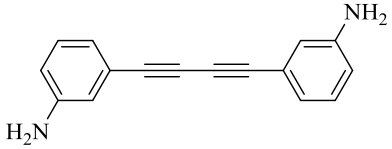
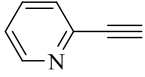
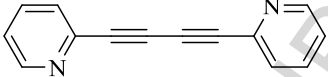
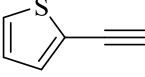
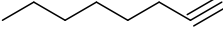
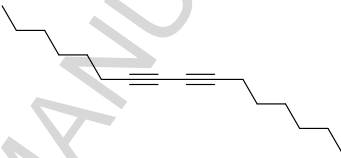
Entry	Catalyst	t(h)	Yield ^b (%)
1 ^c	blank	8	trace
2	CuBr	8	74
3	CuBr ₂	8	10
5	Cu-NPs ^e	8	81
6	Cu ₂ O-NPs ^e	8	70
7	CuO-NPs ^e	8	68
8 ^d	Cu-NPs/Cu ₂ O-NPs	8	80
9	rGO	8	trace
10	Cu ₂ O-rGO	6	83
11	Cu ₂ O-rGO	8	99
12	Cu ₂ O-rGO	10	99
13 ^f	Cu ₂ O-rGO	8	96

^aReaction conditions: phenylacetylene (1mmol), catalyst (4 mg), Cs₂CO₃ (1.2 mmol), EtOH (2 mL), 80 °C, O₂, 8 hours. ^bIsolated yields. ^cCatalyst-free. ^dm(Cu-NPs) : m(Cu₂O-NPs)=1 : 1. ^eCommercial. ^fPhenylacetylene (10 mmol).

Table 2 Cu/Cu₂O-NPs@rGO catalysed homo-coupling of various terminal alkynes^a



Entry	Substrate	Product	Yield ^b (%)
1			99
2			94
3			98
4			96
5			92
6			91
7			90

8			94
9			85
10			83
11			94
12			53

^aReaction conditions: **1** (1 mmol), Cu/Cu₂O-NPs@rGO (4 mg), Cs₂CO₃ (1.2 mmol), EtOH (2 mL), 80 °C, O₂, 8 hours. ^bIsolated yields.

Highlights

- Non-noble Cu/Cu₂O-NPs@rGO catalyzed Glaser homo-coupling.
- Great functional group tolerance.
- The synergic catalysis of Cu/Cu₂O-NPs and graphene.
- Great recyclability.

ACCEPTED MANUSCRIPT